Electroluminescence yield and charge gain in He/CF4 + Iso-butane gas mixtures

Rita Roque, Fernando Amaro, Cristina Monteiro, Joaquim dos Santos, Daniel Mano

LIBPhys-UC

CYGNO

Summary:

An update on the results of the Electroluminescence (EL) yield of gas mixtures containing hydrocarbon gases (iso butane, CH_4,…)

- He/CF_4
- He/CF_4+Iso-butane
- CF_4
- P10

Detector:

A small stainless steal chamber, used in the past for Electroluminescence yield (photons / primary electron) measurements in uniform field (parallel grids gap) and avalanche generated EL (in GEM, THGEM and Micro-Megas).

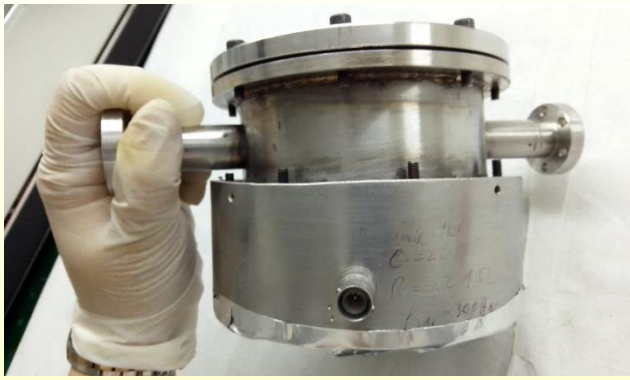

Operated in pure noble gases, using a gas purification and recycling system, based on non evaporable getters.

- Indium sealed.
- Low outgassing materials
- Achieves ~10^{-6} bar before filling with ultra-pure gases

Getters operate at [80,200] ºC (150ºC for CF_4 . Hydrocarbon gases 80ºC)

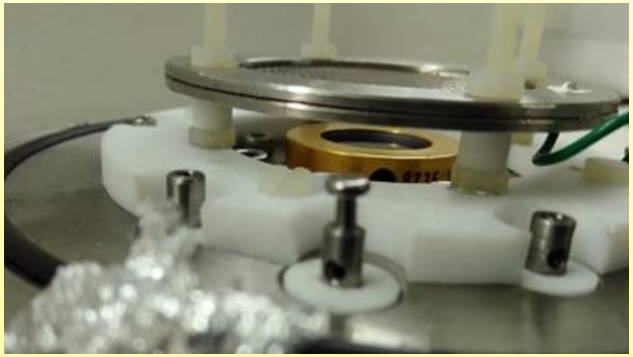

- A. S. Conceição et al., GEM scintillation readout with avalanche photodiodes, JINST P09010, 2007.
- C.M.B. Monteiro et al., Secondary scintillation yield in pure xenon, JINST P05001.(2007)
- C.M.B. Monteiro et al., Secondary scintillation yield in pure argon, Phys. Lett. B 668 (2008)
- Hugo Natal da Luz et al., GEM Operation in High-Pressure CF_4 : Studies of Charge and Scintillation Properties, IEEE TNS, 2009
- C. M. B. Monteiro et al., Electroluminescence from gaseous micropatterned electron multipliers in dark matter detection, Phys. Lett. B, 2009
- C.M.B. Monteiro et al., Secondary scintillation yield from GEM and THGEM gaseous electron multipliers for direct dark matter search, Phys. Lett. B 714 (2012)
- C.A.O. Henriques, et al., "Electroluminescence TPCs at the thermal diffusion limit". JHEP 2019, 27 (2019).

Detector:

A small stainless steal chamber, used in the past for Electroluminescence yield (photons / primary electron) measurements in uniform field (parallel grids gap) and avalanche generated EL (in GEM, THGEM and Micro-Megas).

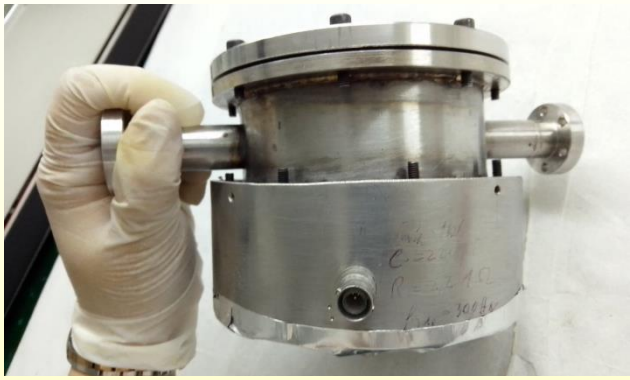

Operated in pure noble gases, using a gas purification and recycling system, based on non evaporable getters.

- Indium sealed.
- Low outgassing materials
- Achieves ~10^{-6} bar before filling with ultra-pure gases

Getters operate at [80,200] ºC (150ºC for CF_4 . Hydrocarbon gases 80ºC)

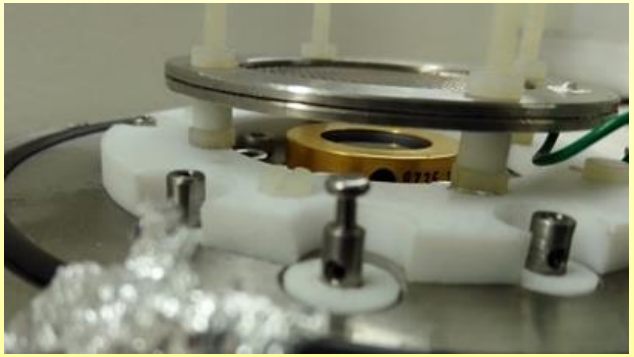

Modified for flow mode:

- Viton seal
- No vacuum before filling
- Getters purification system removed (flow mode)

GEM:

- A standard GEM (50 micron thick, 2.9 x 2.9 cm^2) was used for EL production

Detector setup:

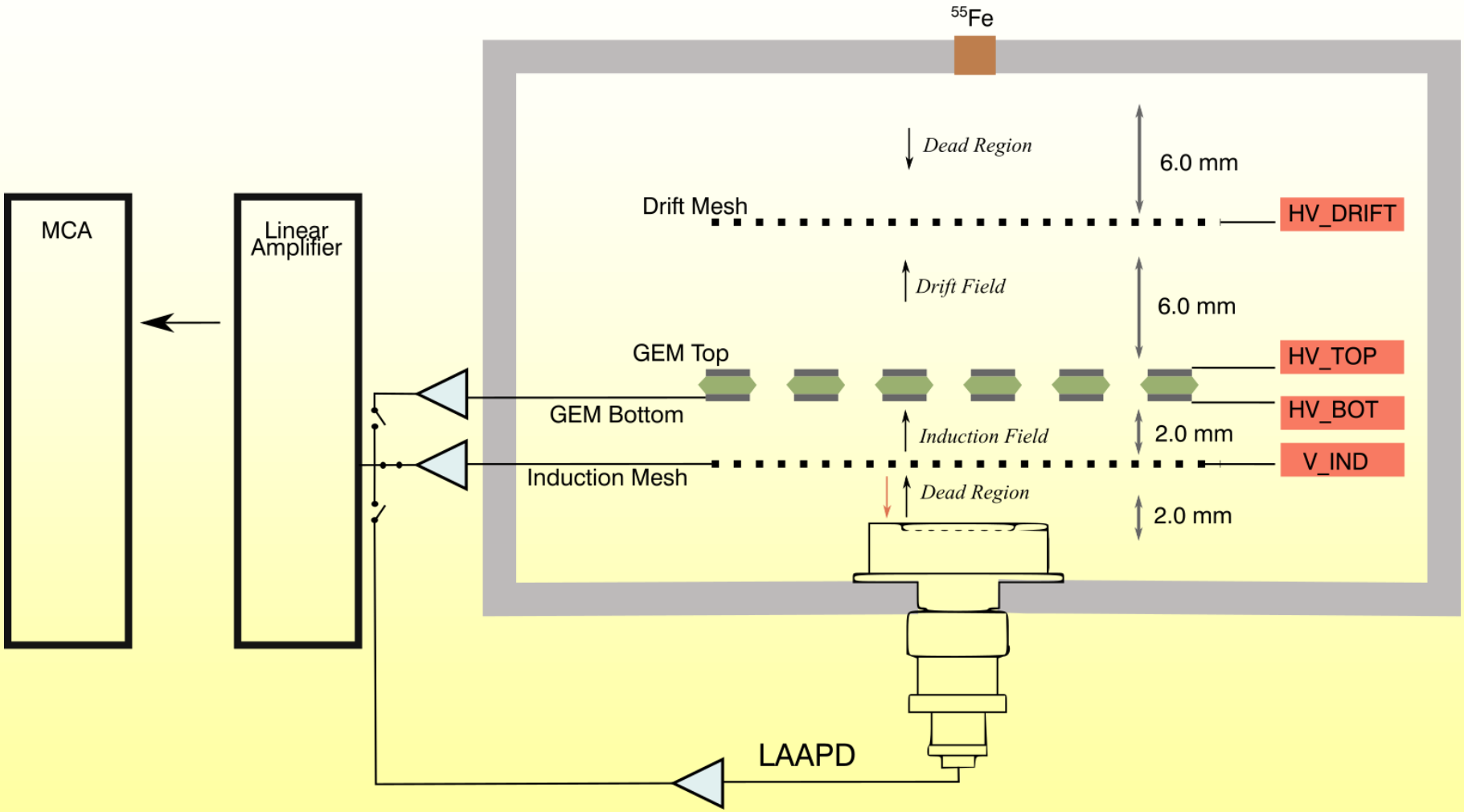

Detector components:

Mesh are made of stainless steel wires (80 micron diameter) with a 900 micron spacing. This results in 84% optical transmission.

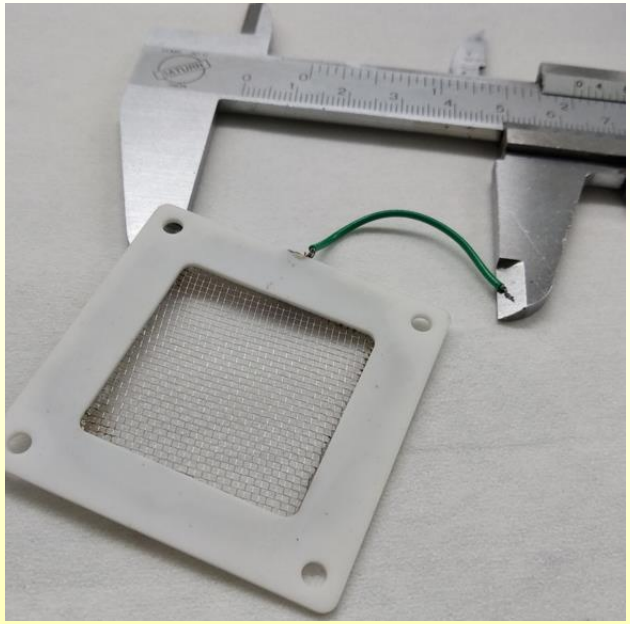

The GEM is a standard one, 2.9x2.9 cm^2

LAAPD:

The LAAPD was made by API (Advanced Photonics Instruments) now LUNA Optoelectronics.

It has 16-mm diameter active area and comes with an SHV connection.

LUNA OPTOELECTRONICS

Non-Cooled Large Area DUV Silicon Avalanche Photodiode

SD 630-70-75-500

WWW.LUNAINC.COM **Precision – Control – Results**

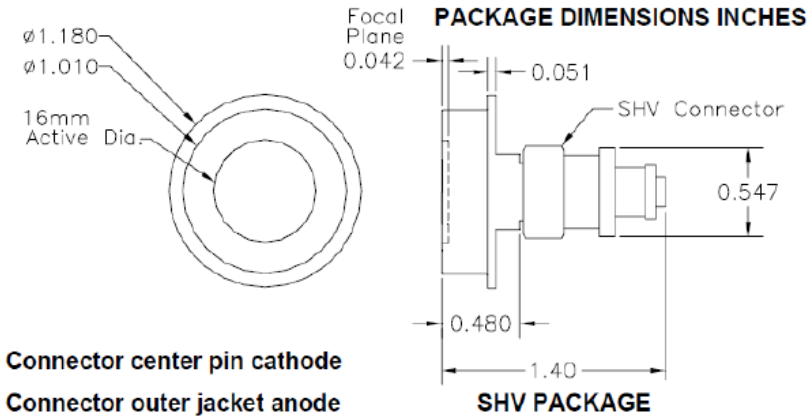

DESCRIPTION

The **SD 630-70-75-500** is a windowless non-cooled large area DUV enhanced silicon avalanche photodiode (APD) with high gain and low noise in a SHV package.

FEATURES

- Low Noise
- High Gain
- High Speed

LAAPD:

The LAPPD sensitivity overlaps the one of the ORCA camera in the visible, but extends down to the deep UV.
We will use a filter to remove the UV component: an N-BK7 optical window will allow to obtain a similar response as the ORCA camera.

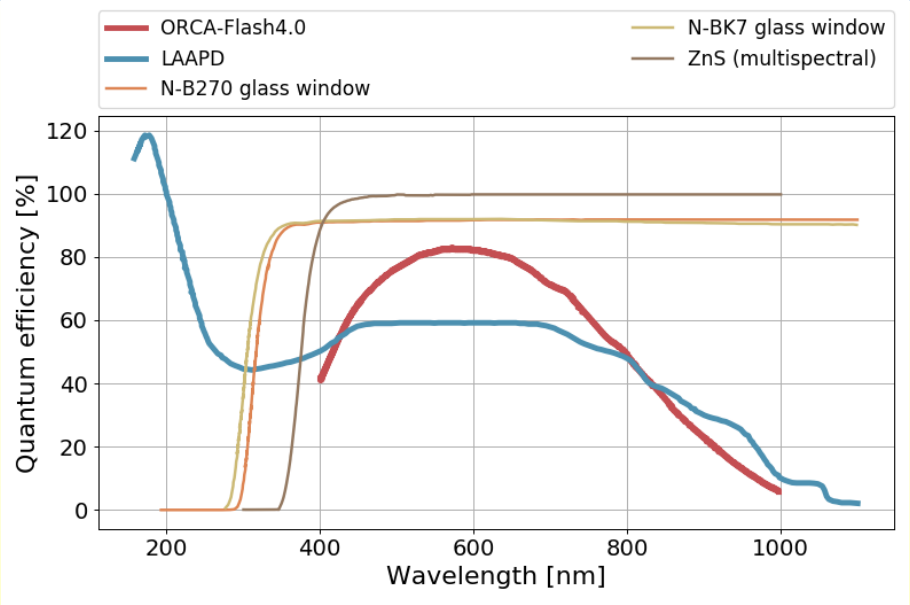

The optical window is not yet installed in our system. As so the results we present cover the spectra down to the VUV.

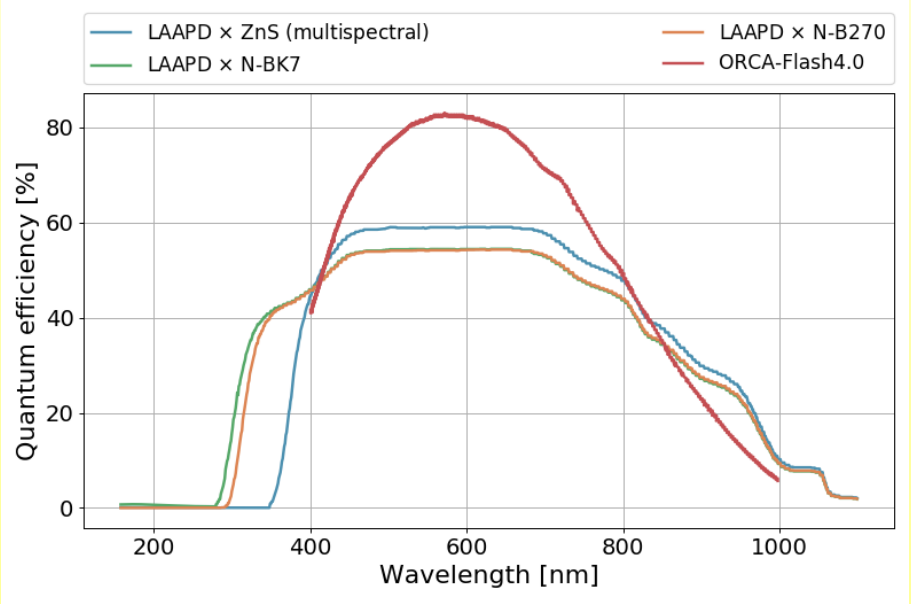

LAAPD:

The LAAPD response comprises two main components:

1) The direct x-rays, which also impinge on the LAAPD and produce a signal. For a given LAAPD biasing, the position of this peak is constant.
2) The Electroluminescence (EL) peak: which depends on the GEM voltage and electric fields in the detector.

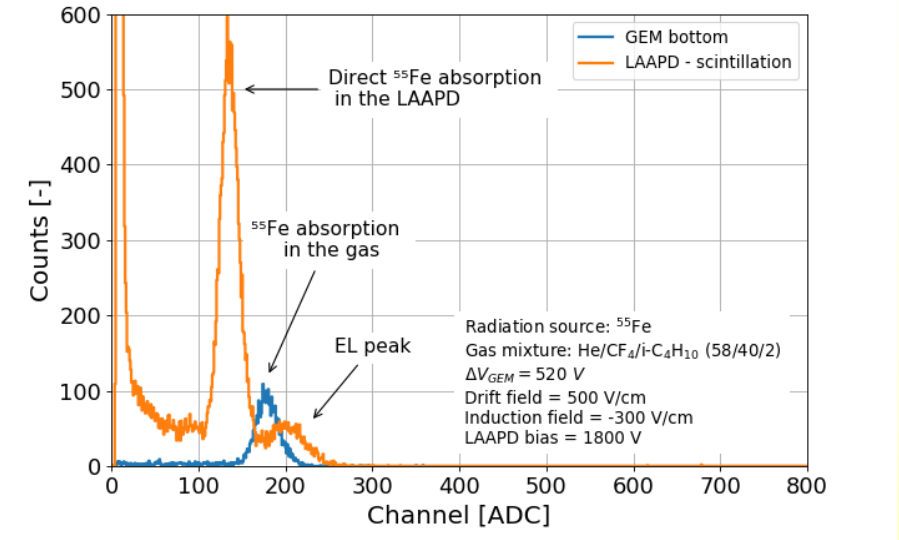

The Electroluminescence Yield is obtained from these 2 components:

$$Y_{\mathrm{EL}} = \frac{\eta_\gamma}{\eta_{e^-}} = \frac{w(\mathrm{gas})}{w(Si)} \times \frac{A_{EL}}{A_X} \times \frac{1}{QE \times \Omega \times T}$$

[photons / primary electron]

A_{EL}, A_X are the centroids of the EL and direct peaks in the LAAPD.
QE used was the value for the plateau at the visible region (0.6)
Ω is the solid angle (0.263)
T is the mesh transparency (84%)

CF_4:

First measurements were done in CF_4, to allow for comparison with previous work (with gas recirculation and purification with getters) :

- The charge gains are spot on
- The GPM (GEM + LAAPD) gain drops by a small factor: expected, since the gas purity has influence over the EL yield. Main effect should be in the VUV.

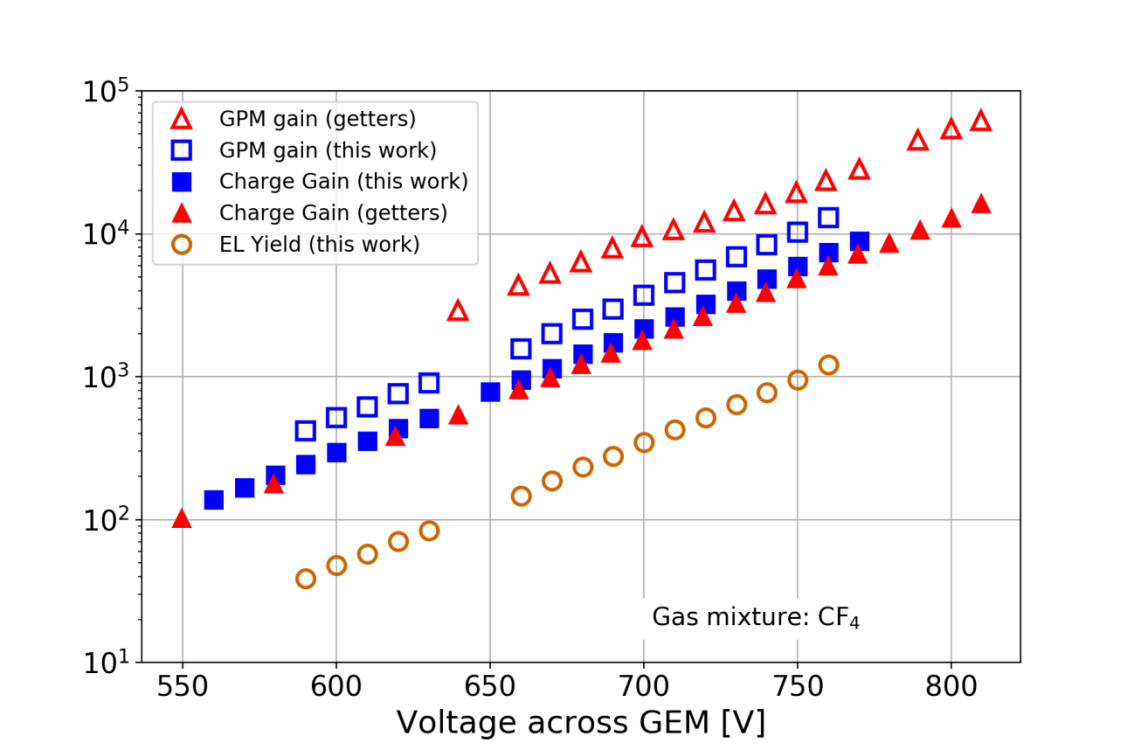

Hugo Natal da Luz et al., GEM Operation in High-Pressure CF_4 : Studies of Charge and Scintillation Properties, IEEE TNS, 2009

CF_4: Drift Region Optimization

During the drift region optimization we encountered a unexpected behavior:

The charge gains measured on the GEM continued to increase with the drift field for longer than anticipated (no plateau). The El yield (LAAPD) followed the same behavior.

(decrease in the primary electron recombination during the drift)

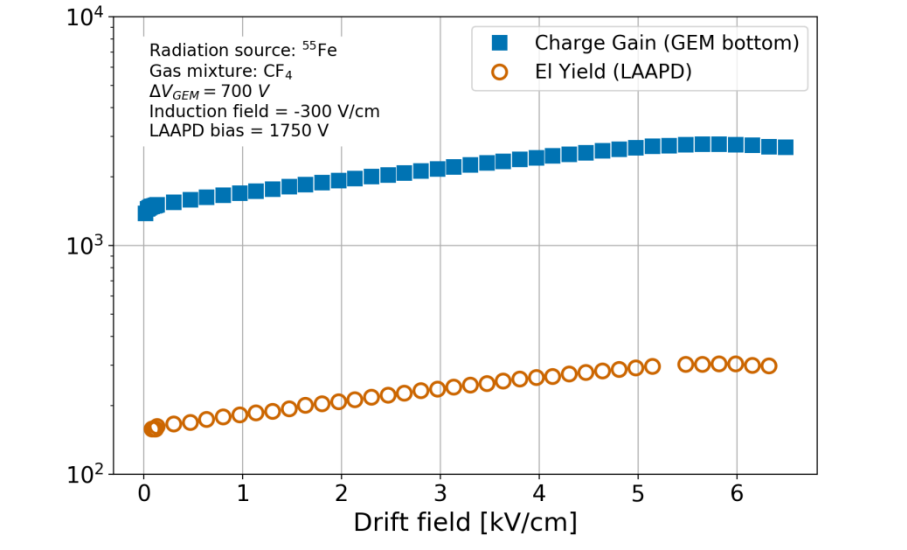

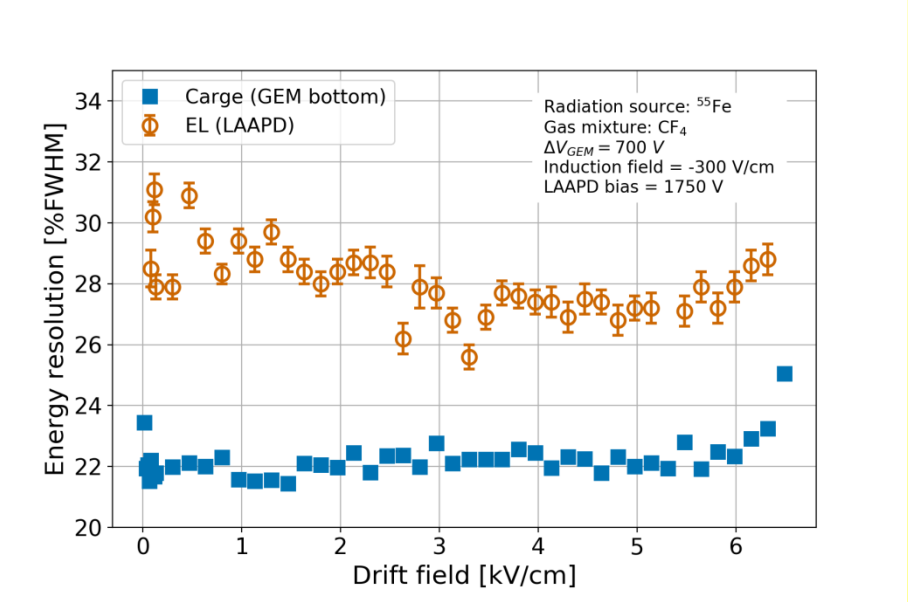

CF_4: Drift Region Optimization

During the drift region optimization we encountered a unexpected behavior:

The charge gains measured on the GEM continued to increase with the drift field for longer than anticipated (no plateau). The El yield (LAAPD) followed the same behavior.

A test with P10 showed a more typical behavior, so it is indeed caused by the gas (and not some issue with the detector).

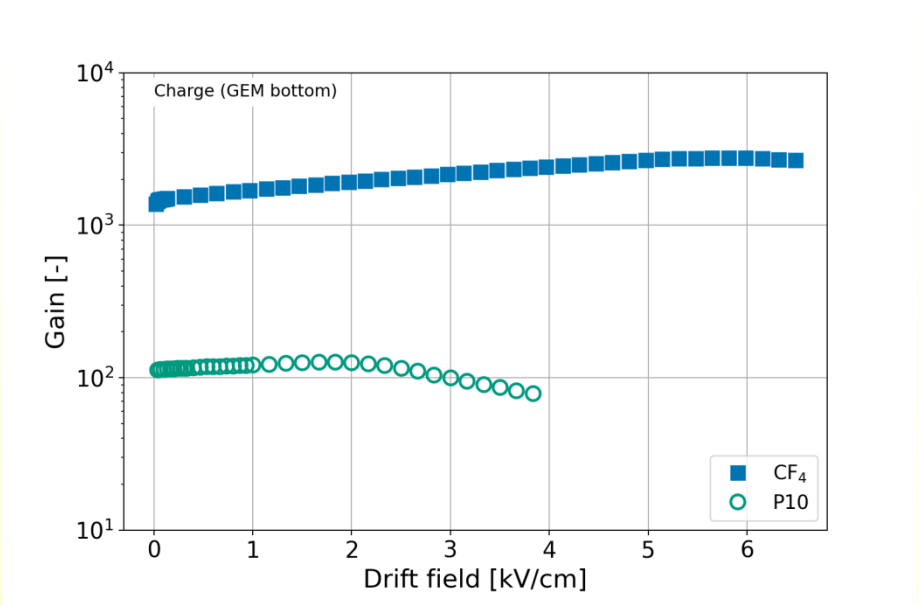

CF_4: GEM gain

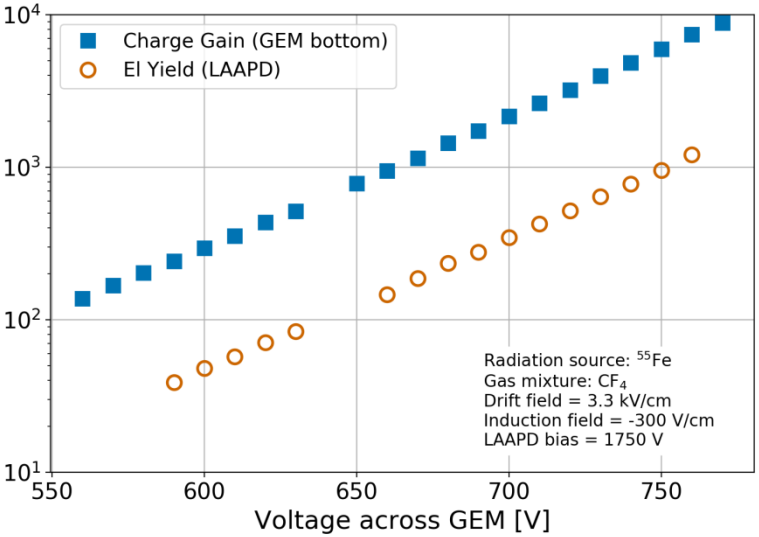
Charge Gain (GEM bottom)
El Yield (LAAPD)
Radiation source: ^{55}Fe
Gas mixture: CF_4
Drift field = 3.3 kV/cm
Induction field = -300 V/cm
LAAPD bias = 1750 V
Voltage across GEM [V]

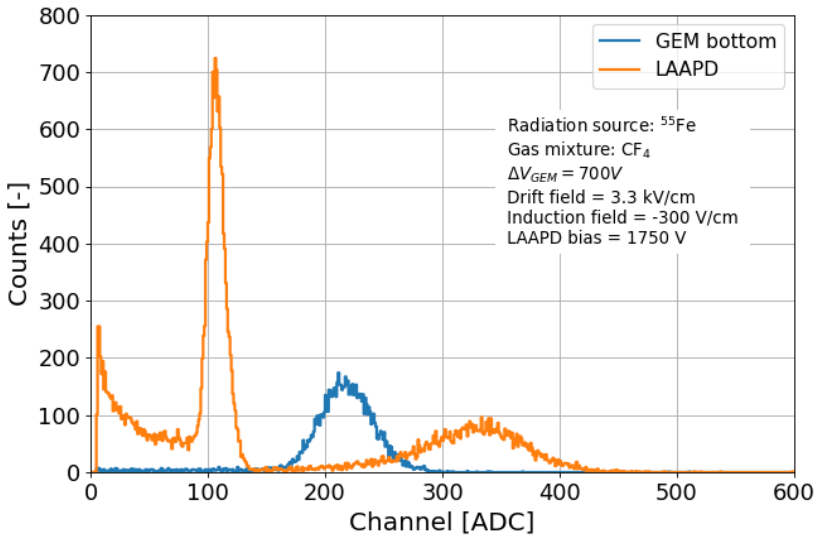
GEM bottom
LAAPD
Radiation source: ^{55}Fe
Gas mixture: CF_4
$\Delta V_{GEM} = 700V$
Drift field = 3.3 kV/cm
Induction field = -300 V/cm
LAAPD bias = 1750 V
Counts [-]
Channel [ADC]

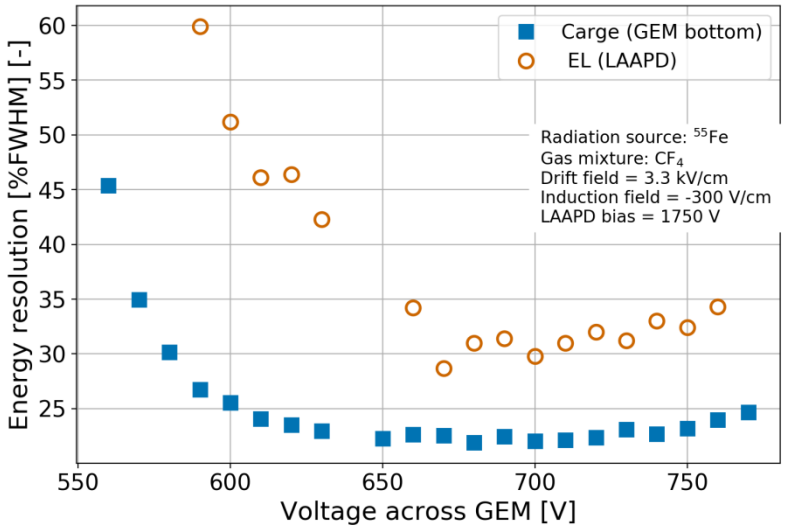
Carge (GEM bottom)
EL (LAAPD)
Radiation source: ^{55}Fe
Gas mixture: CF_4
Drift field = 3.3 kV/cm
Induction field = -300 V/cm
LAAPD bias = 1750 V
Energy resolution [%FWHM] [-]
Voltage across GEM [V]

CF_4: Induction field

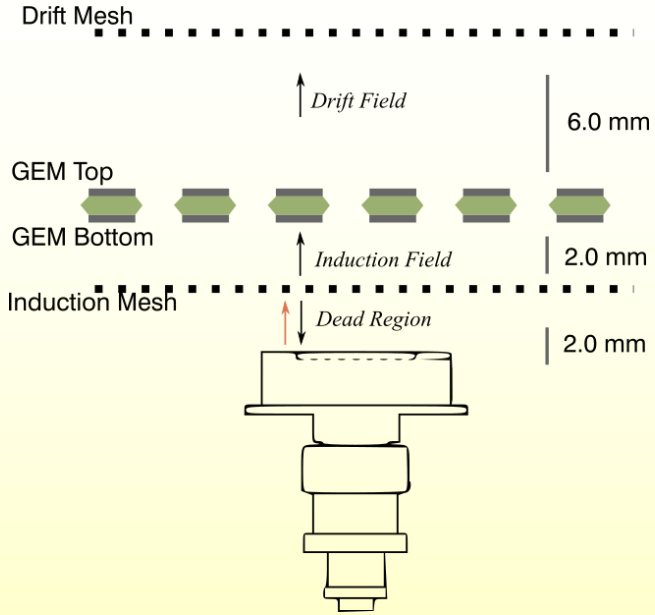

Previous results were taken with a negative (in respect to figure) Induction field, to ensure all the charge was collected at the GEM Bottom.

For this study, we vary the induction field and collect the signals on the GEM Bottom and on the Induction Mesh.

The induction field was changed by changing the voltages on the GEM Bottom while also changing the ones on GEM Top and Drift Mesh (to keep those fields constant).

Another surprise was the behavior of the GEM Bottom signal after 7 kV/cm: showing an increase (?)

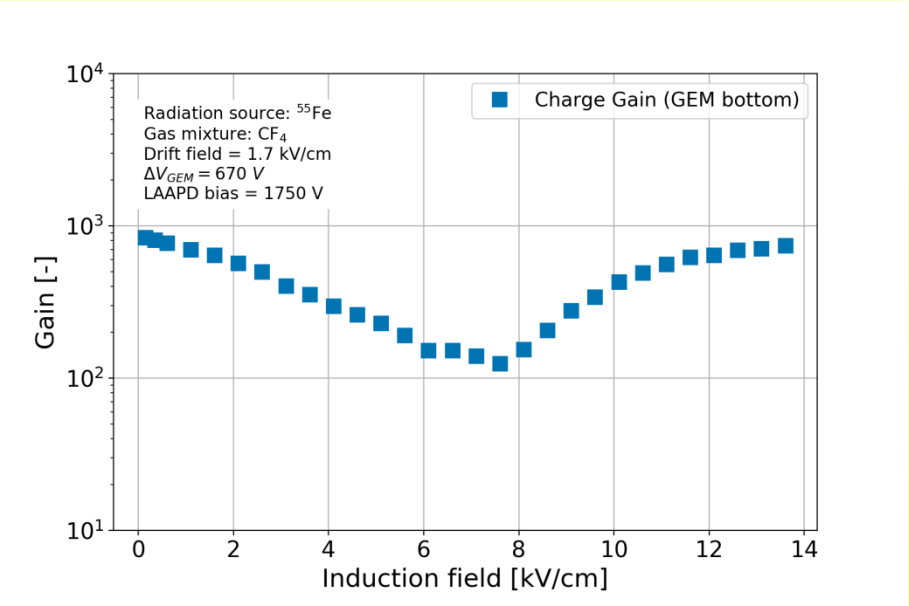

CF_4: Induction field

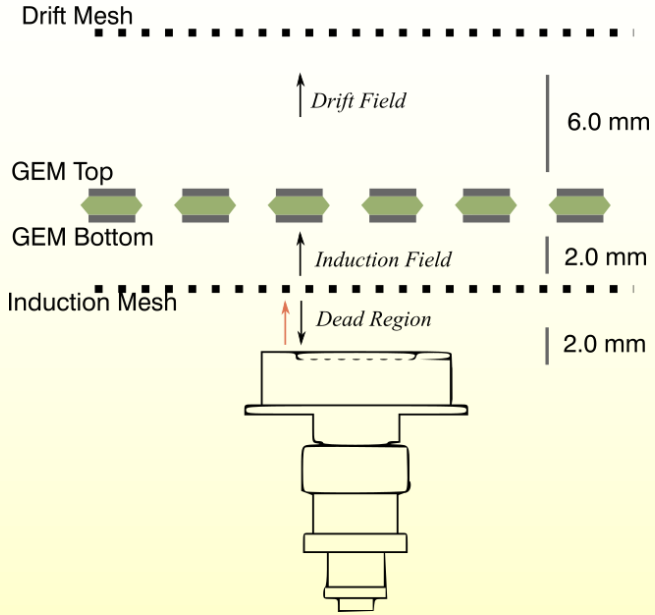

Previous results were taken with a negative (in respect to figure) Induction field, to ensure all the charge was collected at the GEM Bottom.

For this study, we vary the induction field and collect the signals on the GEM Bottom and on the Induction Mesh.

The induction field was changed by changing the voltages on the GEM Bottom while also changing the ones on GEM Top and Drift Mesh (to keep those fields constant).

Another surprise was the behavior of the GEM Bottom signal after 7 kV/cm: showing an increase (?)

For the same region of Induction Field, the signal on the induction mesh, which as expected had been increasing, started to present a drop.

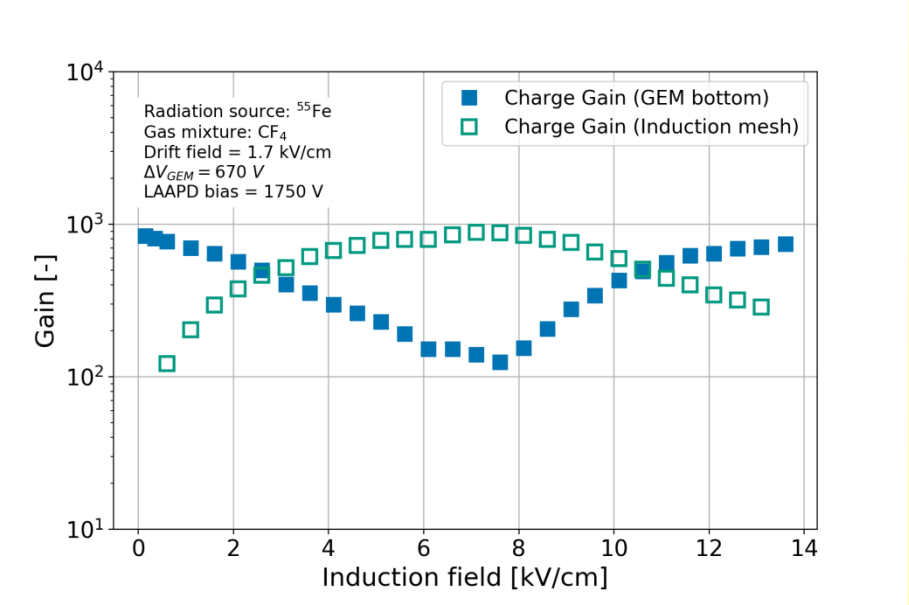

CF_4: Induction field

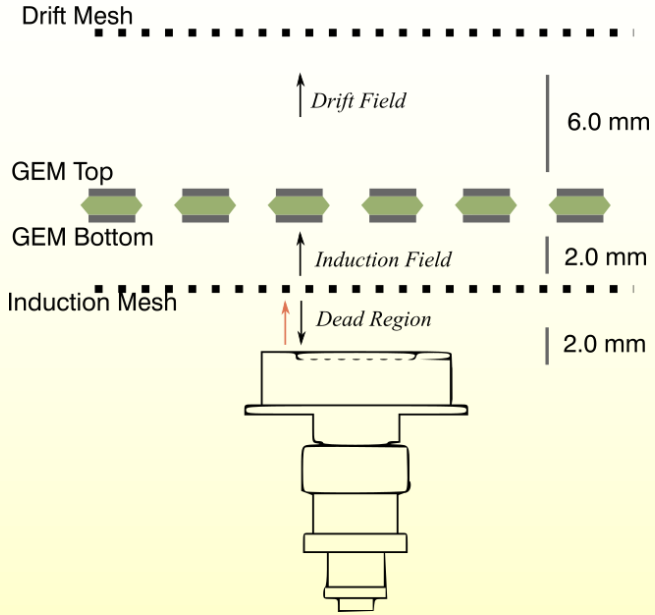

Previous results were taken with a negative (in respect to figure) Induction field, to ensure all the charge was collected at the GEM Bottom.

For this study, we vary the induction field and collect the signals on the GEM Bottom and on the Induction Mesh.

The induction field was changed by changing the voltages on the GEM Bottom while also changing the ones on GEM Top and Drift Mesh (to keep those fields constant).

Another surprise was the behavior of the GEM Bottom signal after 7 kV/cm: showing an increase (?)

For the same region of Induction Field, the signal on the induction mesh, which as expected had been increasing, started to present a drop.

The sum of the 2 components (total charge) increases slightly.

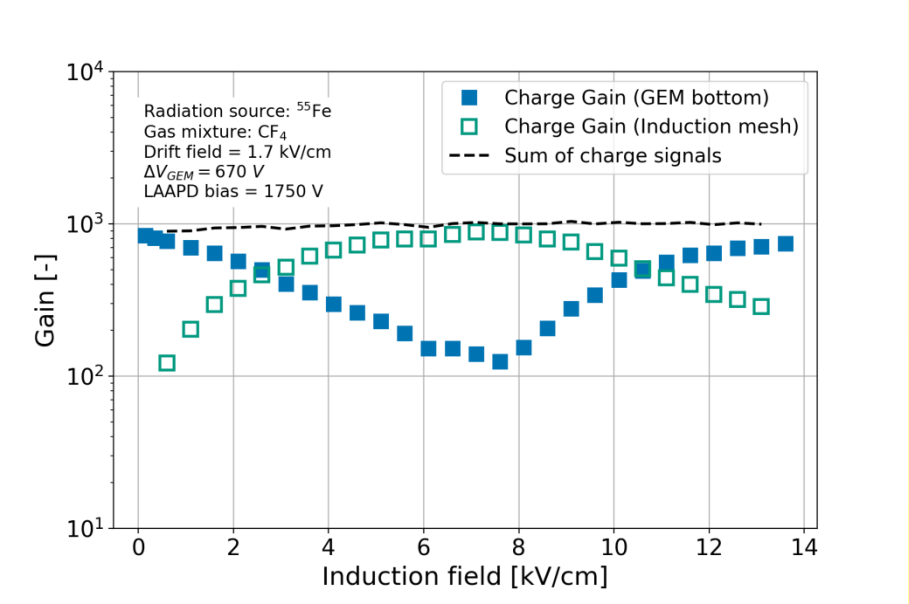

CF_4: Induction field

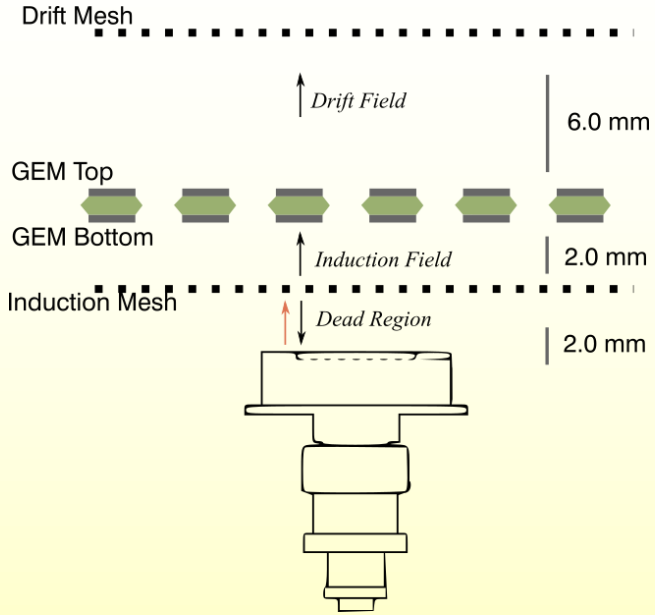

Previous results were taken with a negative (in respect to figure) Induction field, to ensure all the charge was collected at the GEM Bottom.

For this study, we vary the induction field and collect the signals on the GEM Bottom and on the Induction Mesh.

The induction field was changed by changing the voltages on the GEM Bottom while also changing the ones on GEM Top and Drift Mesh (to keep those fields constant).

Another surprise was the behavior of the GEM Bottom signal after 7 kV/cm: showing an increase (?)

For the same region of Induction Field, the signal on the induction mesh, which as expected had been increasing, started to present a drop.

The sum of the 2 components (total charge) increases slightly.

The same for the Electroluminescence Yield.

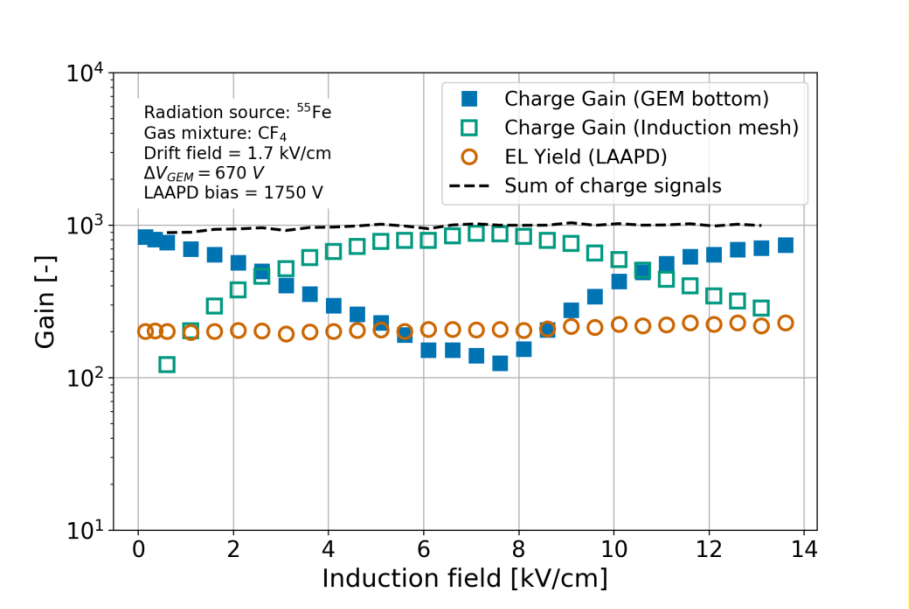

P10: Induction field

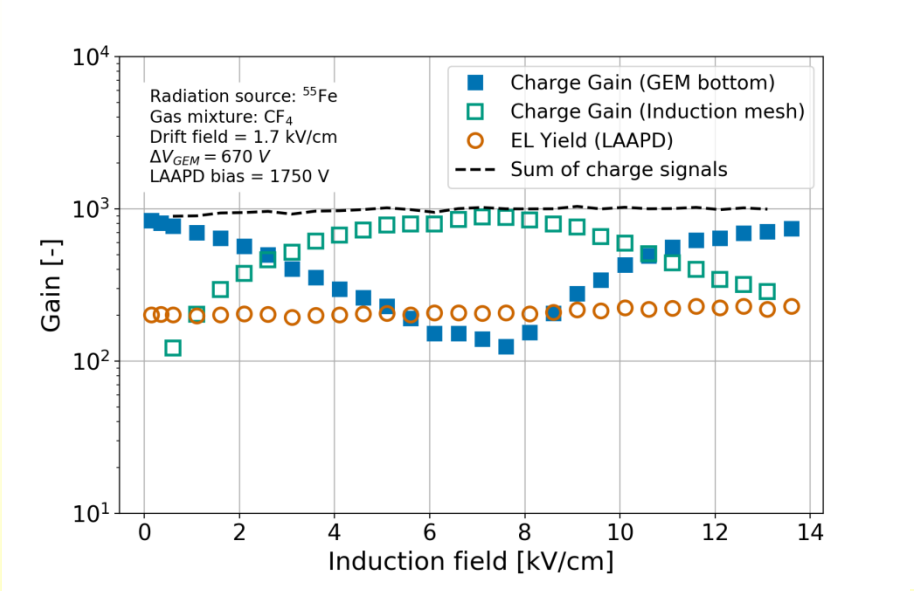

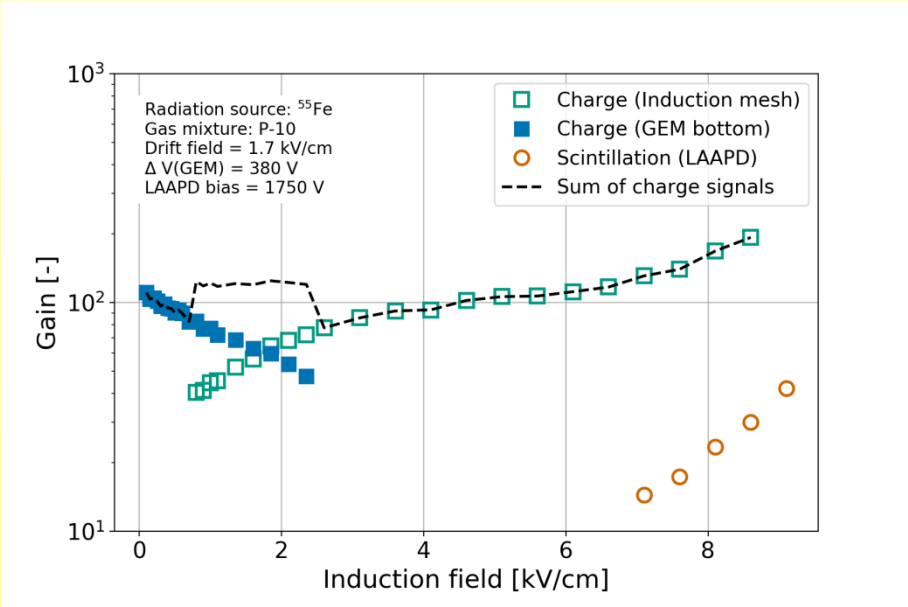

The behavior in P10 was very different:

- The signal on the GEM bottom decreases its amplitude with the increase in the induction field the signal
- The signal on the induction mesh increases steadily.
- <u>Above 7 kV/cm, we observe some EL with the LAAPD</u>

CF_4: Induction field

The pulse height distributions are relatively normal and do not present any major feature:

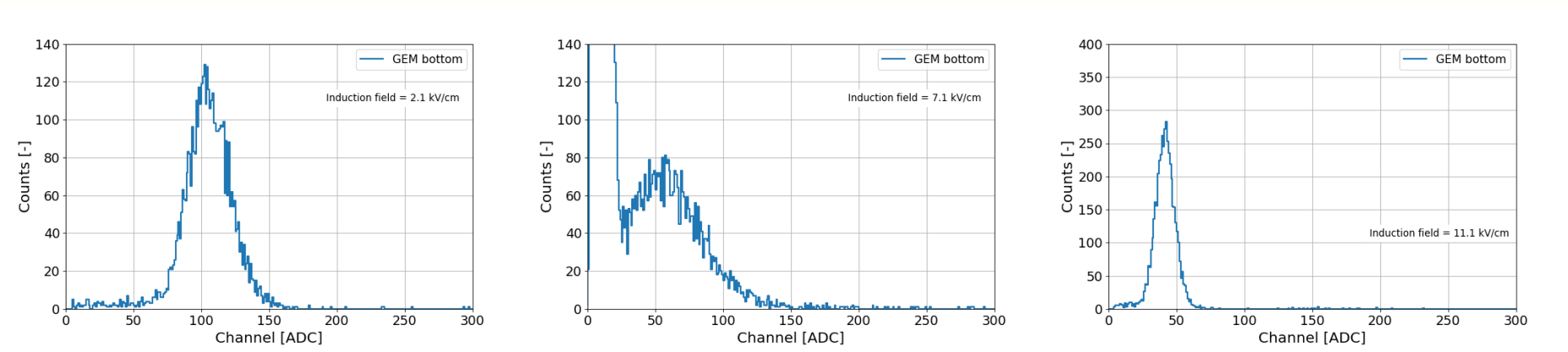

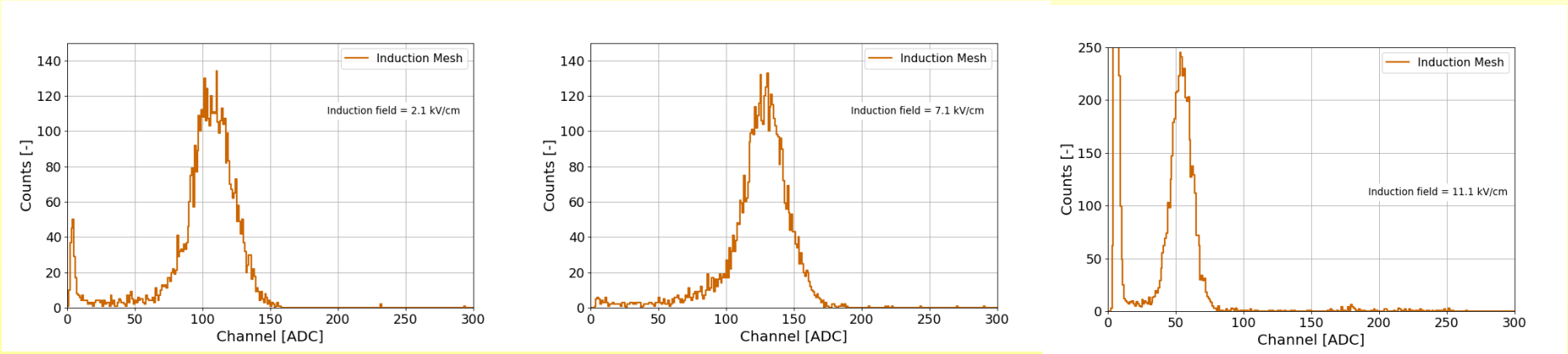

He/CF_4 (60/40): Induction field

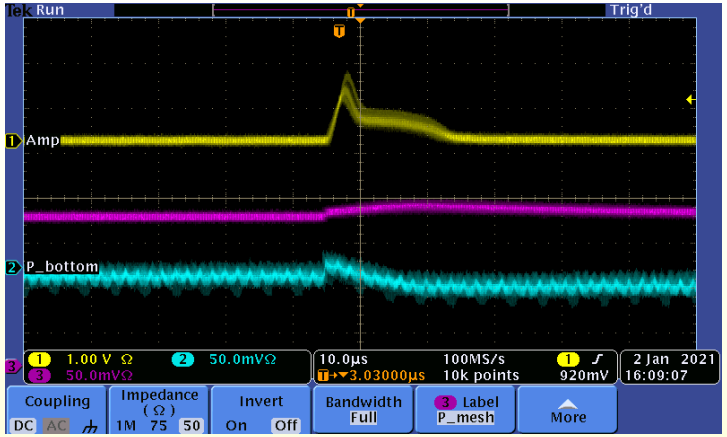

Are ions contributing to the signal at higher induction fields?

Gem Bottom = positive ions

Mesh = negative ions

More detailed studies will be done

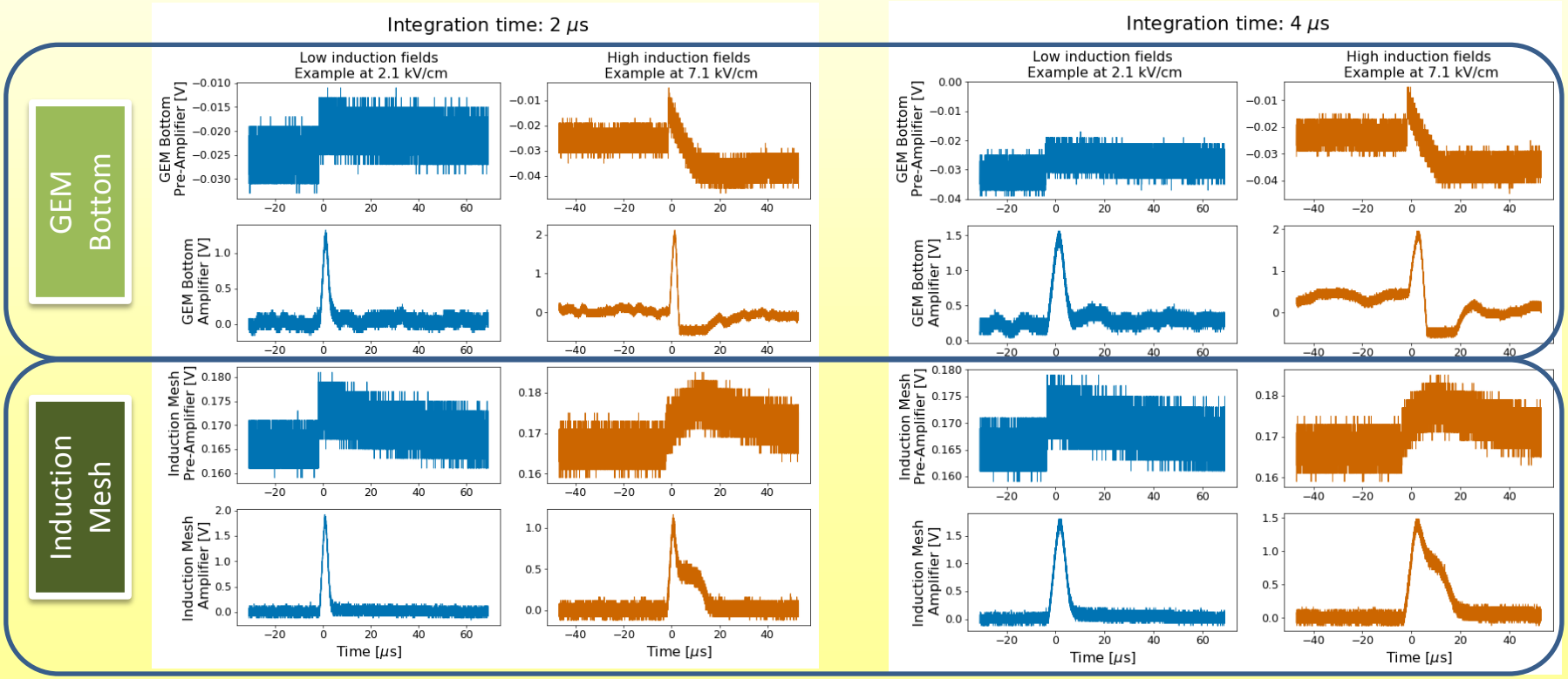

He/CF_4 (60/40)

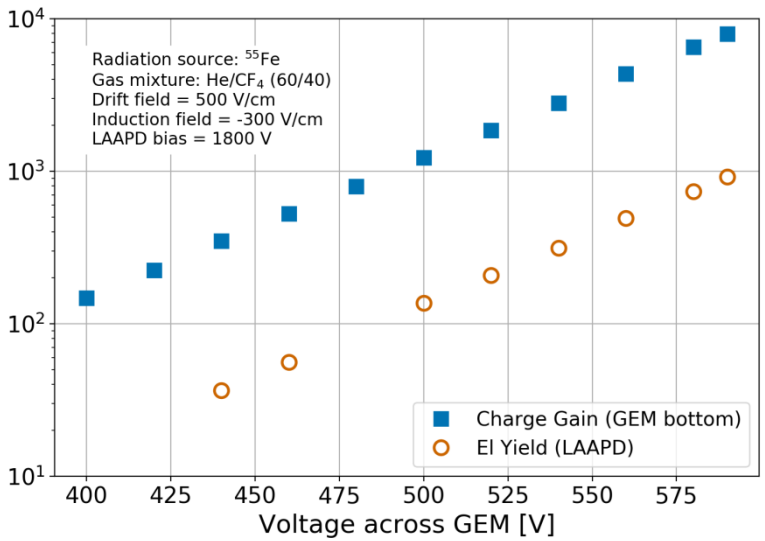
Radiation source: ^{55}Fe
Gas mixture: He/CF_4 (60/40)
Drift field = 500 V/cm
Induction field = -300 V/cm
LAAPD bias = 1800 V
Charge Gain (GEM bottom)
El Yield (LAAPD)
10^4
10^3
10^2
10^1
400 425 450 475 500 525 550 575
Voltage across GEM [V]

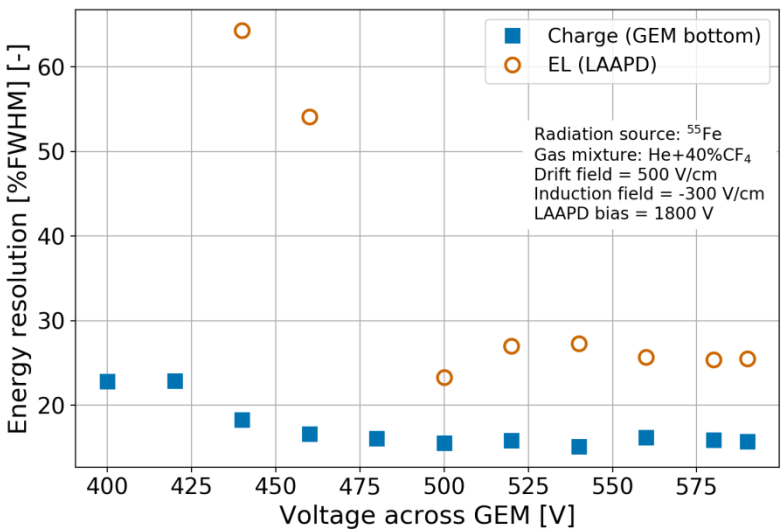
Charge (GEM bottom)
EL (LAAPD)
Radiation source: ^{55}Fe
Gas mixture: $He+40\%CF_4$
Drift field = 500 V/cm
Induction field = -300 V/cm
LAAPD bias = 1800 V
Energy resolution [%FWHM] [-]
20 30 40 50 60
400 425 450 475 500 525 550 575
Voltage across GEM [V]

He/CF_4 (60/40) vs CF_4

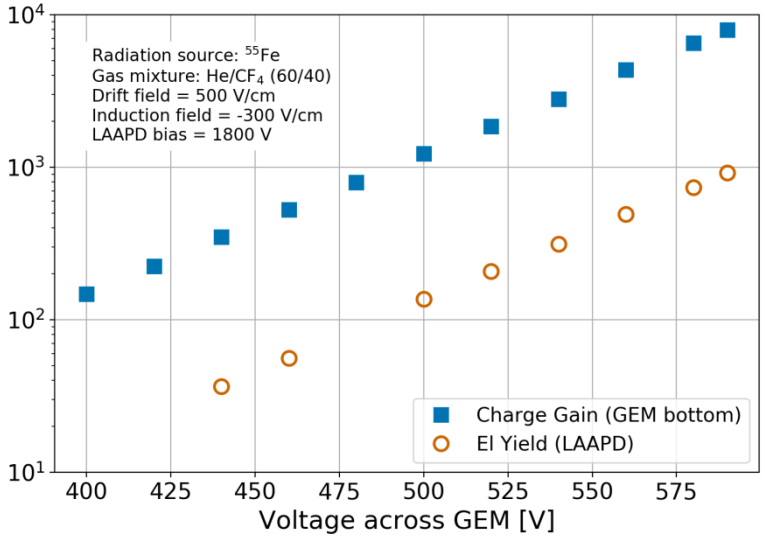

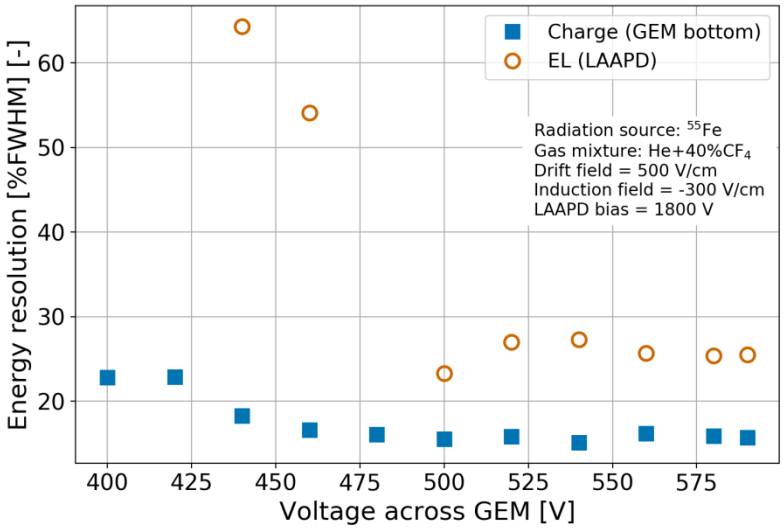

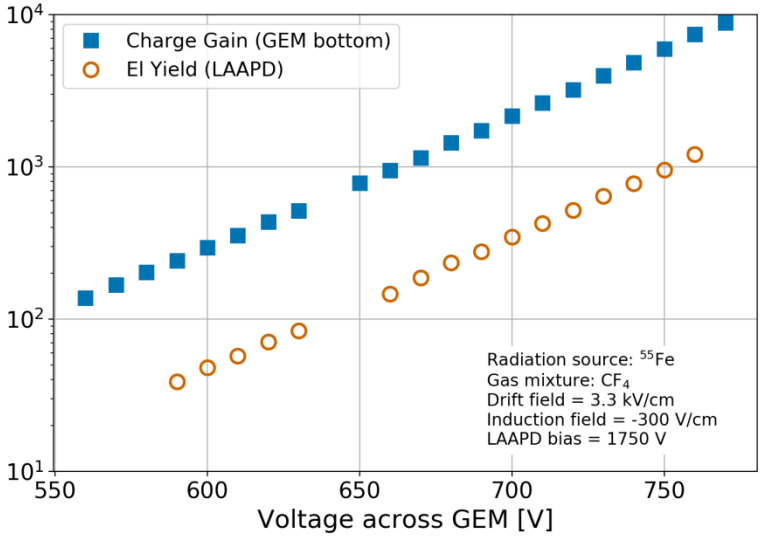

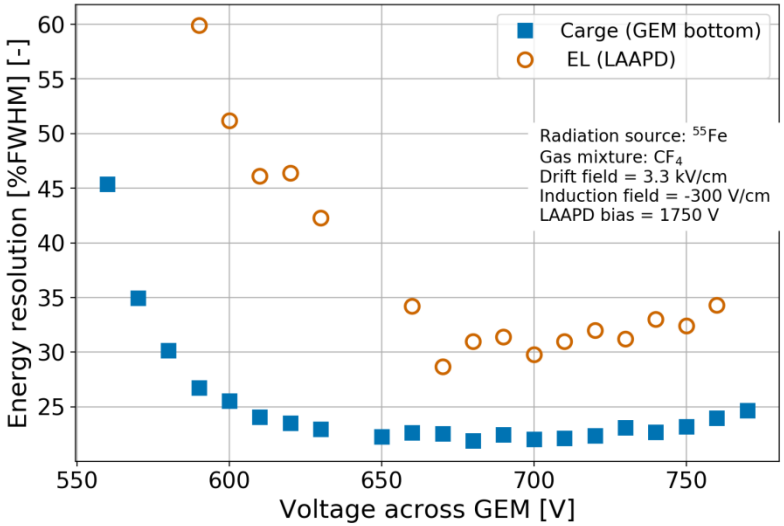

He/CF_4 (60/40): induction field

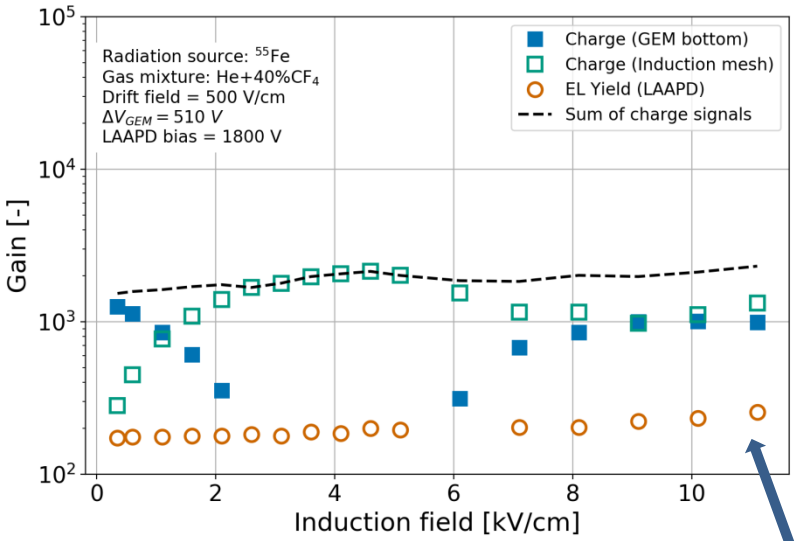

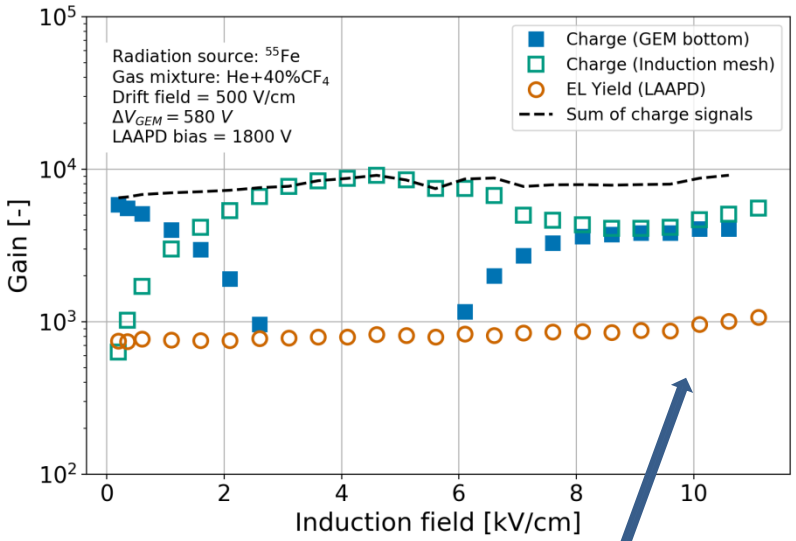

We seem to observe adition EL production in the induction gap, starting at fields around 10 kV/cm.
Discharges prevented us to continue the measurements

He/CF_4 (60/40) vs CF_4

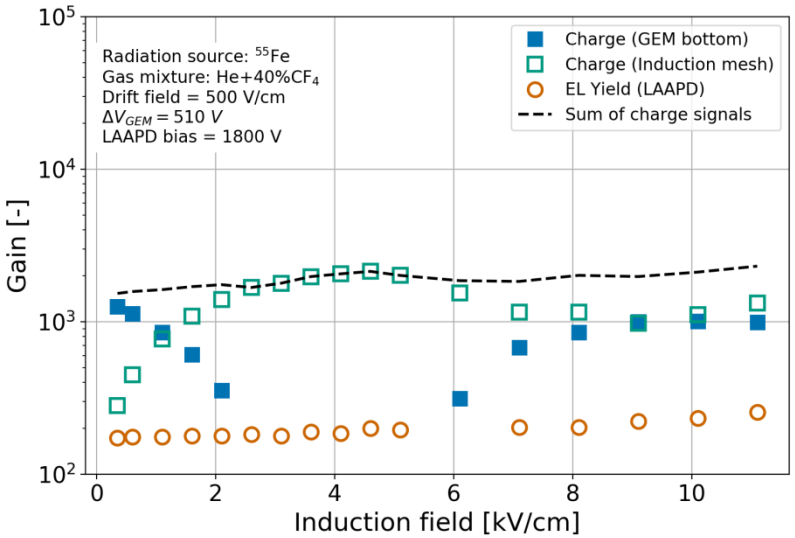

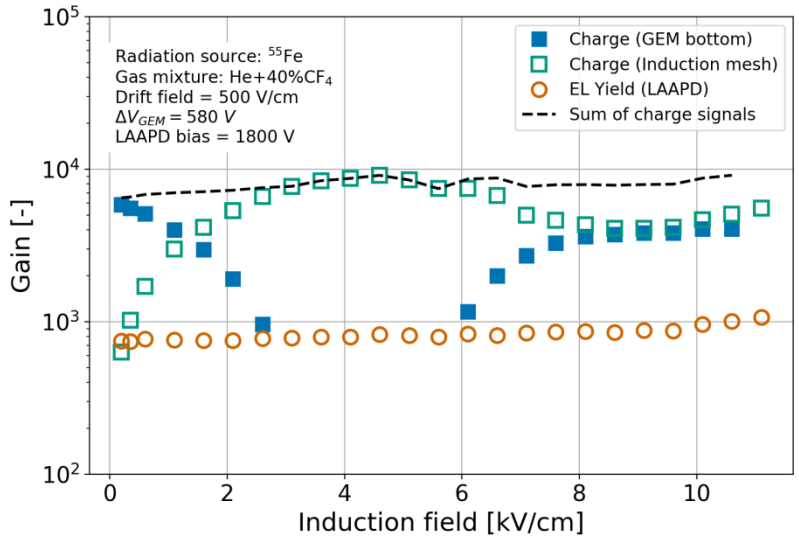

This was not the case with CF_4

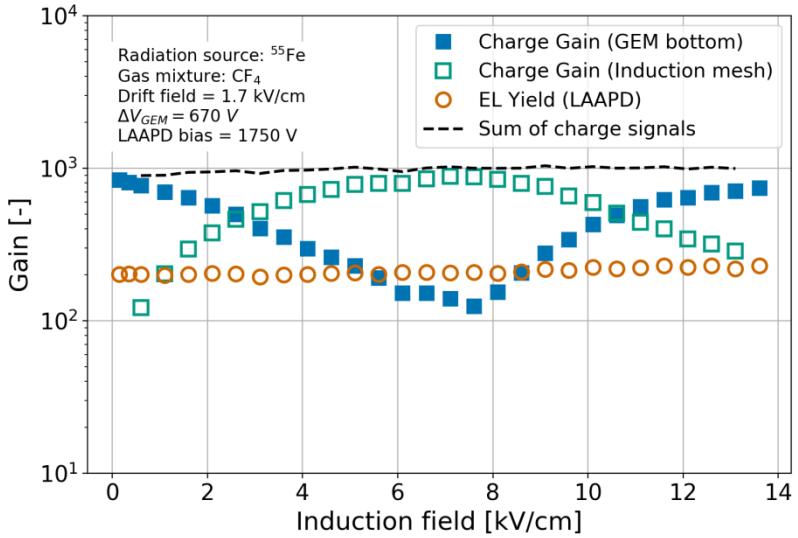

He/CF_4/Iso-Butane (58/40/2)

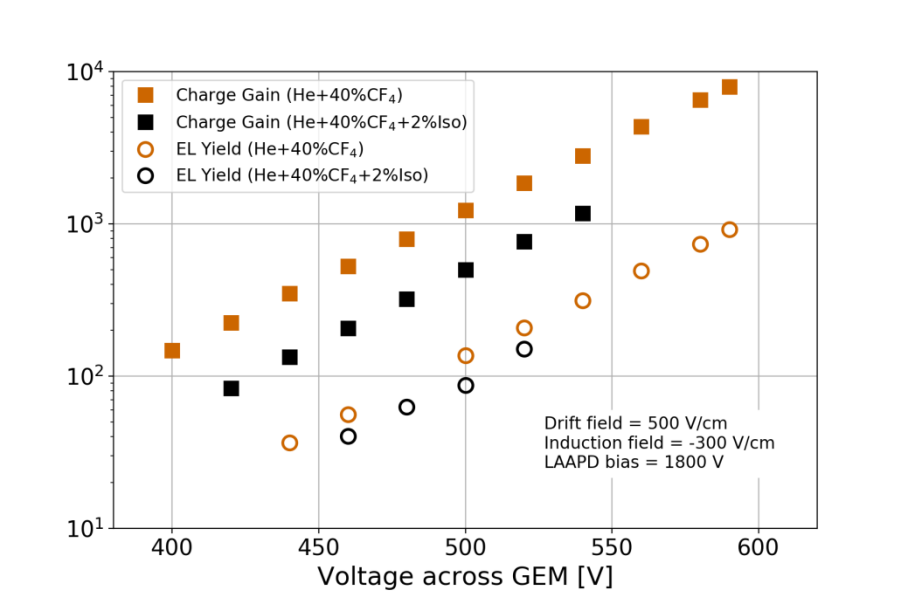

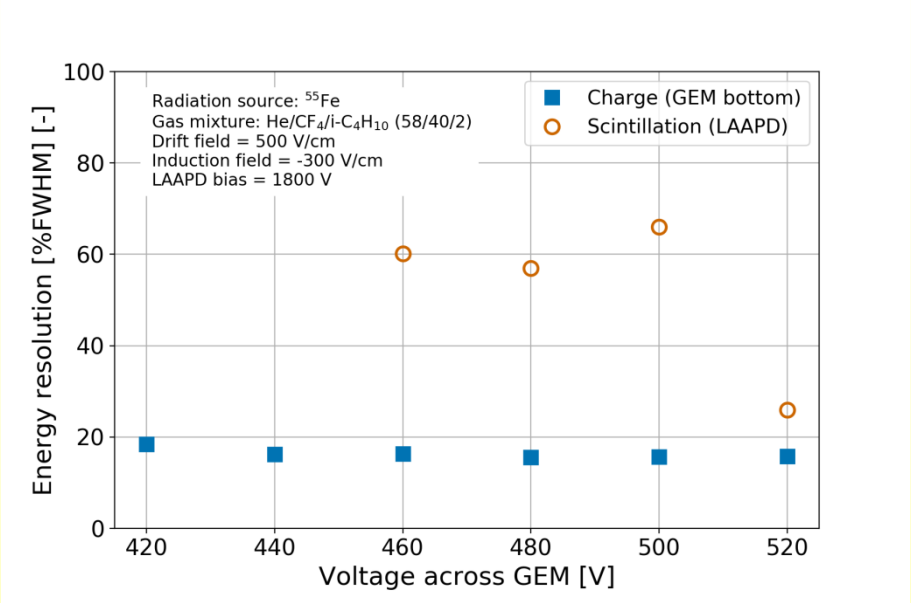

Onset of discharges sooner with the inclusion of Iso-butane

He/CF_4/Iso-Butane (58/40/2)

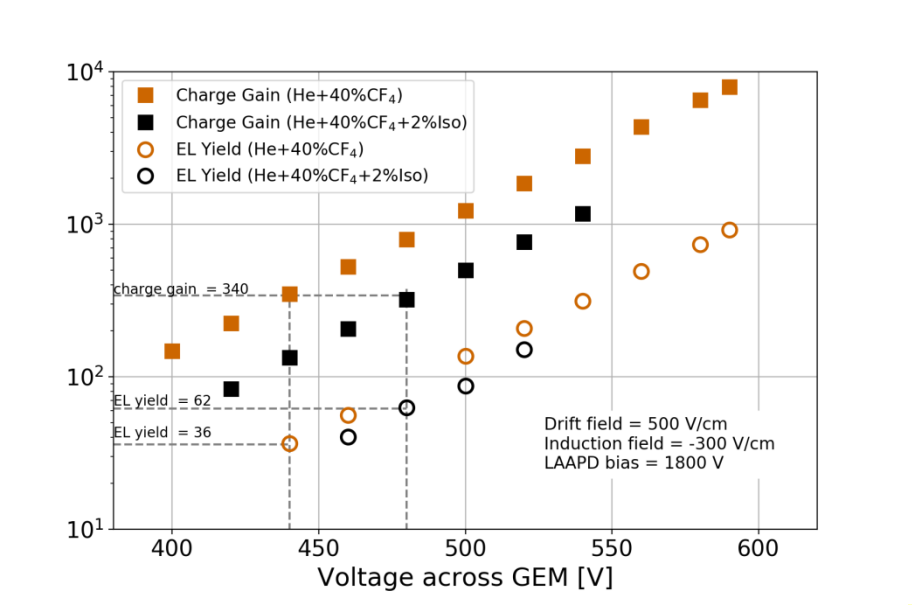

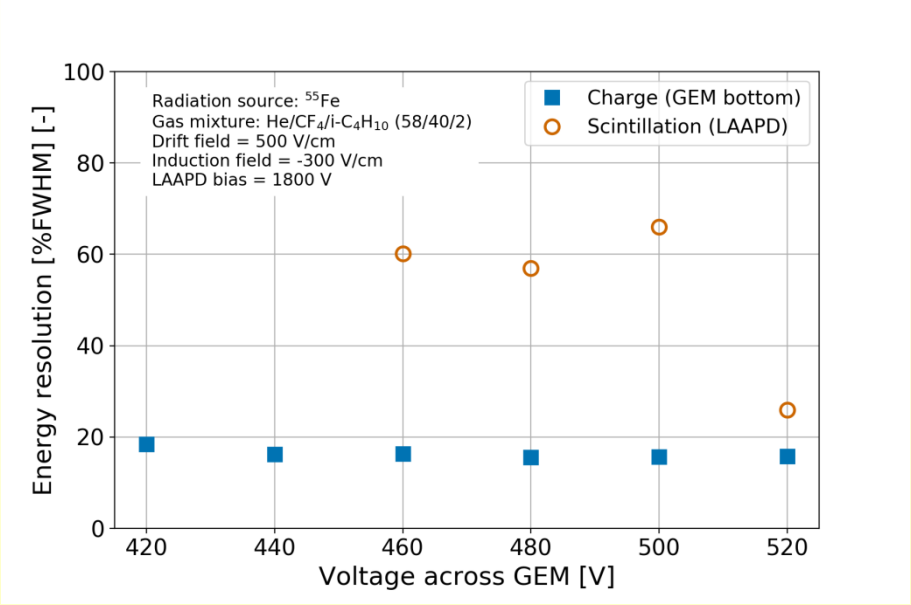

For same charge gain, higher EL yield in He/CF4/Iso (58/40/2) ?

To do list:

- Change iso-butante % in the He/CF_4/iso mix
- Investigate behaviour of the GEM bottom and induction mesh signals in the CF_4 mixtures with drift and induction fields (ions contributing to signal?)
- Improve detector insulation in order to achieve higher induction fields
- Include optical glass window for VUV component removal
- Return to operation in sealed mode (using getters)

He/CF_4/Iso-Butane (58/40/2)

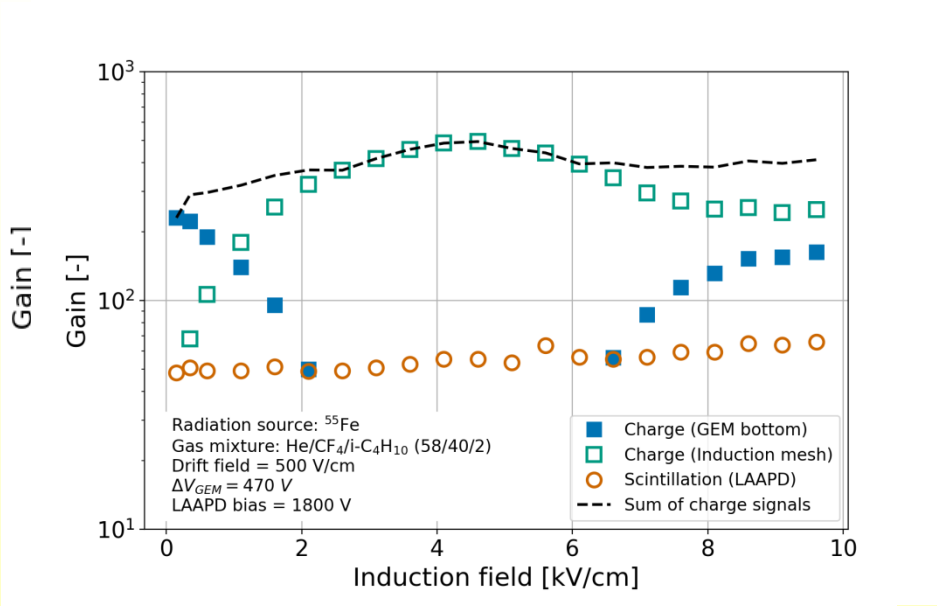

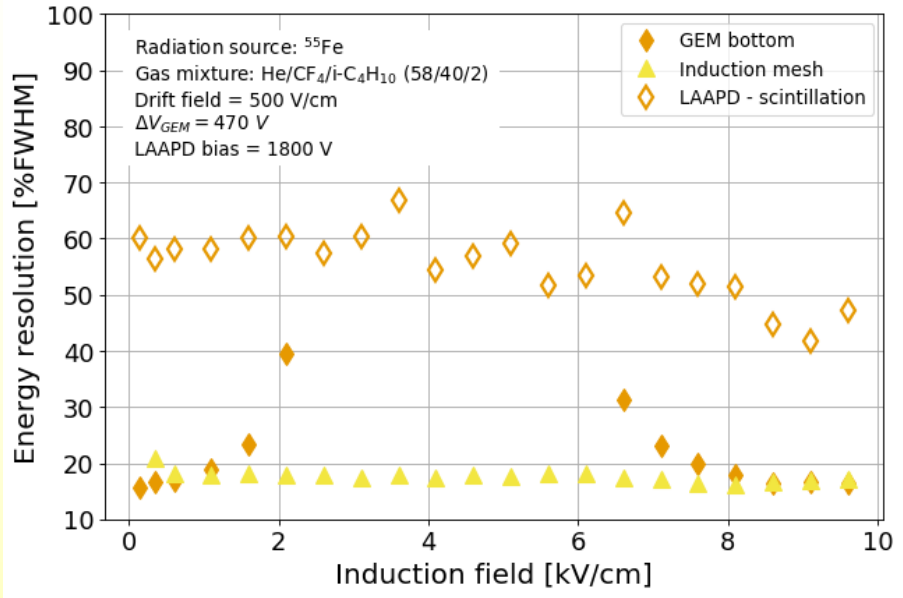

He/CF_4/Iso-Butane (58/40/2)

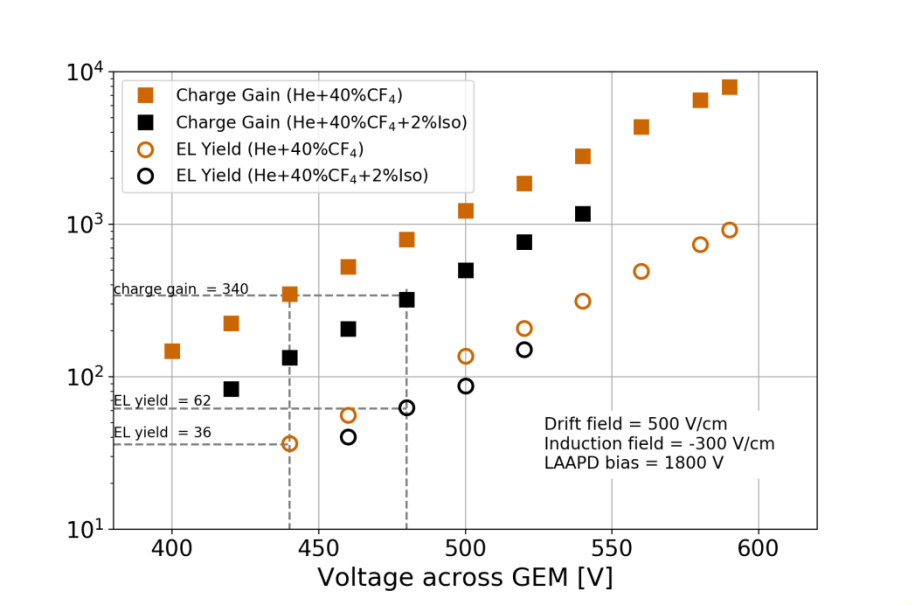

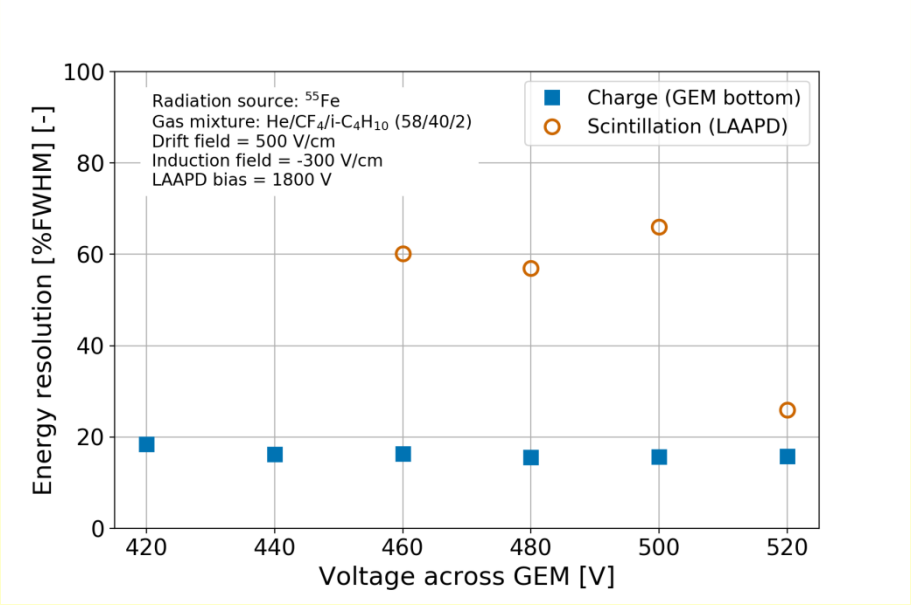

For same charge gain, higher EL yield in He/CF4/Iso (58/40/2) ?

- W values of the mixtures are wrong?

Material	w -value (eV)
Si	3.2
He	41
CF_4	54
Iso-Butane	23
He/CF_4	46,2
He/CF_4/Iso	45,84

Archana Sharma, Properties of some gas mixtures used in tracking detectors

He/CF_4/Iso-Butane (58/40/2)

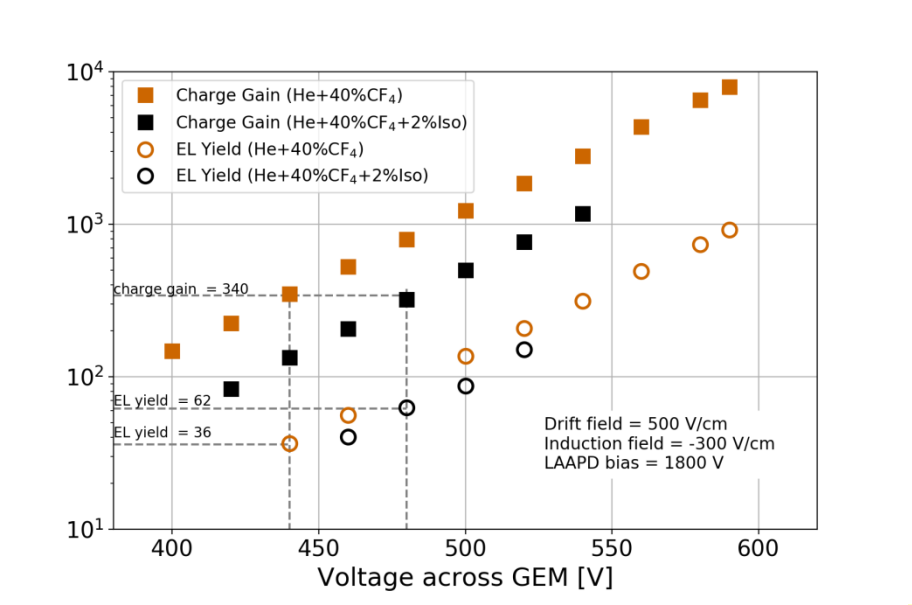

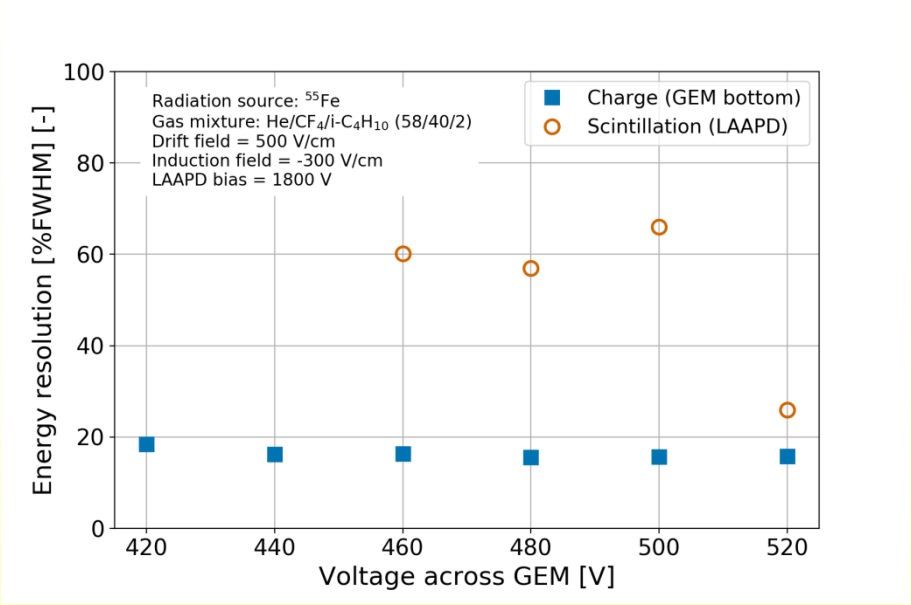

For same charge gain, higher EL yield in He/CF4/Iso (58/40/2) ?

- W values of the mixtures are wrong?
- Electric fields are not the optimal for the He/CF4/iso ?

Material	w -value (eV)
Si	3.2
He	41
CF_4	54
Iso-Butane	23
He/CF_4	46,2
He/CF_4/Iso	45,84

Archana Sharma, Properties of some gas mixtures used in tracking detectors

LAAPD: EL Yield calculation

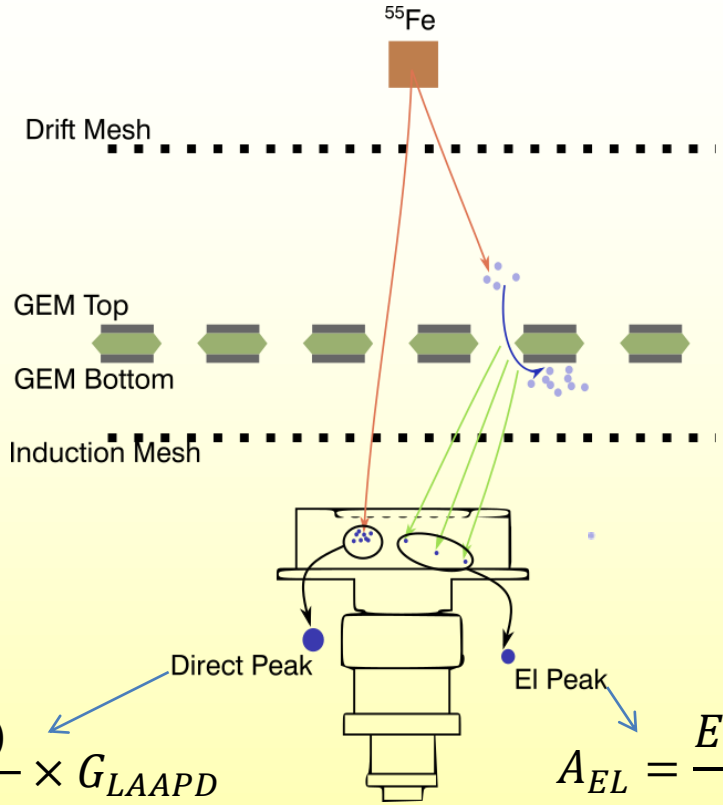

$$A_X = \frac{E(5.9keV)}{W_{Si}} \times G_{LAAPD}$$

$$A_{EL} = \frac{E(5.9keV)}{W_{gas}} \times Y_{EL} \times \Omega \times T \times QE \times G_{LAAPD}$$

$$Y_{\mathrm{EL}} = \frac{\eta_\gamma}{\eta_{e^-}} = \frac{w(\mathrm{gas})}{w(Si)} \times \frac{A_{EL}}{A_X} \times \frac{1}{QE \times \Omega \times T}$$

[photons / primary electron]

AEL, AX are the scintillation and direct peaks centroids in the LAAPD.

He/CF_4 (60/40)

E_{IND} = 2.1 kV/cm

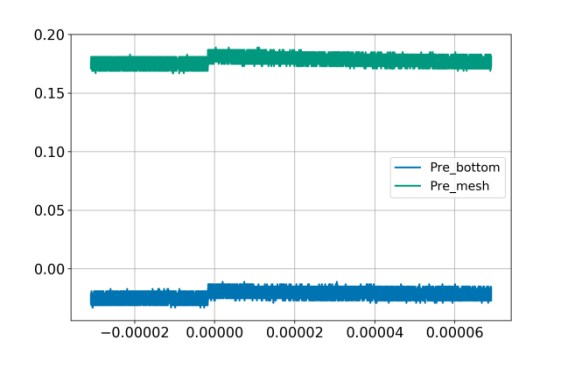

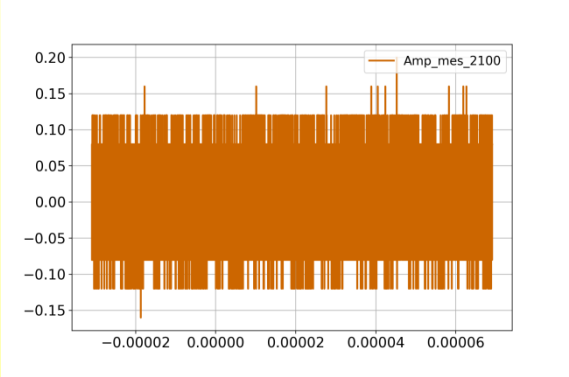

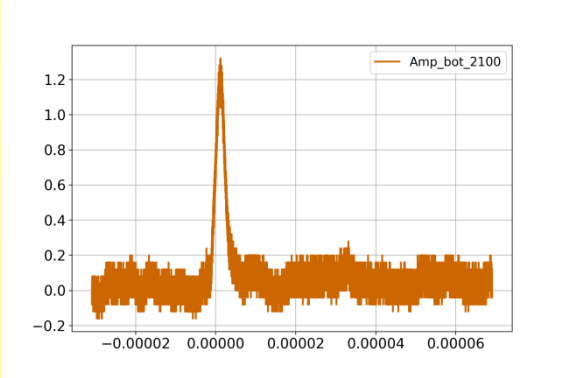

E_{IND} = 5.1 kV/cm

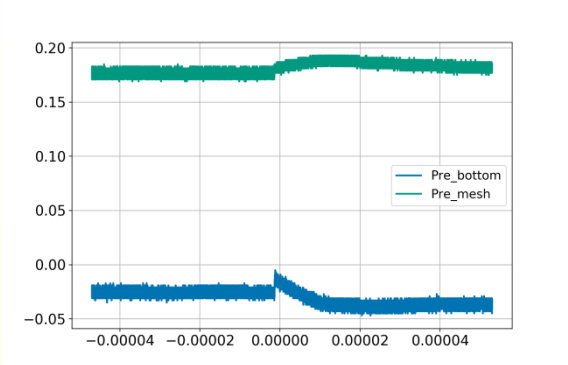

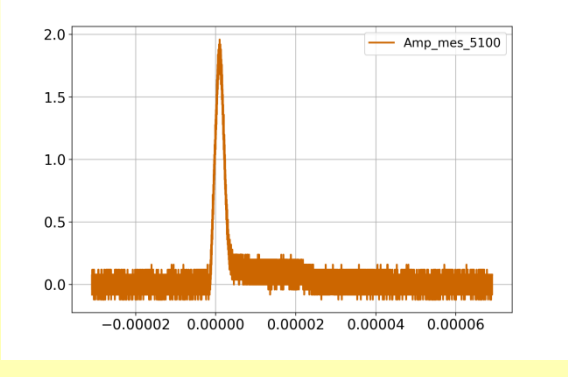

E_{IND} = 7.1 kV/cm